HORSESHOE IN A CLASS OF PLANAR MAPPINGS

YAN HUANG AND XIAO-SONG YANG

Bursting dynamics of mappings is investigated in this paper. We first present stability analysis of the mappings' equilibria with various parameters. Then for three mappings P, $\bar{P}$, and $\hat{P}$ with different parameters, we study their powers P^4, $\bar{P}^6$, and $\hat{P}^4$. We show that the mappings thus obtained are chaotic by giving a rigorous verification of existence of horseshoes in these mappings. Precisely, we prove that the mapping $\bar{P}^6$ is semiconjugate to the 3-shift mapping; the mappings P^4 and $\hat{P}^4$ are semiconjugate to the 4-shift mapping.

1. Introduction

Bursting is ubiquitous in physical and biological systems, especially in neural systems [3]. Studying networks of bursters in neural systems poses challenging mathematical problems. Even simulating such networks is a computational challenge, since thousands of stiff nonlinear ordinary differential equations (ODEs) may be involved.

Bursting dynamics of mappings has recently been investigated by physicists [1, 5, 6, 2]. Using a discrete-time system, say $x_{n+1} = f(x_n)$, instead of a system of ODEs, provides one with a number of theoretical and computational advantages. For example, it is possible to explore collective behavior of millions of coupled discrete-time bursters with only modest computational effort.

In order to study the phenomenon of bursting, a simple discrete-time model of spiking neurons was proposed in [3], which is of the following form:

$$\text{I:} \quad \begin{aligned} v_{n+1} &= 0.04v_n{}^2 + 6v_n + 140 - u_n + I, \\ u_{n+1} &= 0.004v_n + 0.98u_n, \end{aligned}$$

$$\text{if } v_n \geq 30mV, \quad \text{then} \begin{cases} v_n \longleftarrow c, \\ u_{n+1} \longleftarrow u_n + d. \end{cases} \tag{1.1}$$

In this paper, we study a more general mapping as follows.

Let $l = 0.04$, $n = 6$, $\bar{I} = 41$, (1.1) can be rewritten as follows:

$$\text{II:} \quad \begin{aligned} v_{n+1} &= 0.04v_n^2 + 6v_n + 41 - u_n, \\ u_{n+1} &= av_n + bu_n, \end{aligned} \tag{1.2}$$

$$\text{if } v_n \geq 30mV, \quad \text{then} \begin{cases} v_n \longleftarrow c, \\ u_{n+1} \longleftarrow u_n + d. \end{cases} \tag{1.3}$$

Depending on the values of the parameters, this mapping can produce a variety of bursting patterns [3]. In addition, this simple model can reproduce 20 most fundamental neuron-computational properties of biological spiking neurons summarized in [3].

2. The stability of equilibria with various parameters

We first study in this section the stability of equilibria of (1.2) for different parameters.

Equation (1.2) has two equilibria, let A and B denote them. Let the modules of the eigenvalues of A be m_{11} and m_{12}, the modules of the eigenvalues of B be m_{21} and m_{22}. m_{11}, m_{12}, m_{21}, and m_{22} vary with the parameters a and b as shown in Figure 2.1, $m_{i,j} = m_{i,j}(a,b)$, $i,j = 1,2$. Denote by M the plane $z = 1$ in Figure 2.1. With the reference plane M, it can be concluded that A is a saddle point when a and b vary from 0 to 0.99, respectively, and B may be a saddle point, a stable equilibrium, or an unstable equilibrium when a and b varies from 0 to 0.99.

Typical values for c and d are $c = -56$, $d = -16$. When $a = 0.24$ and $b = 0.6$, let P denote the mapping II. The mapping P has two saddle points $(-10.2786, -6.1672)$ and $(-99.7214, -59.8328)$. When $a = 0.64$ and $b = 0.2$, let $\bar{P}$ denote the mapping II, the mapping $\bar{P}$ has a saddle point $(-10.8917, -8.7134)$ and a stable equilibrium $(-94.1083, -75.2866)$.

In the next section, we recall a result on horseshoes theory developed in [8, 9], which is essential for rigorous verification of existence of chaos in the systems discussed in this paper.

3. Review of a topological horseshoe theorem

Let X be a metric space, D is a compact subset of X, and $f : D \rightarrow X$ is mapping satisfying the assumption that there exist m mutually disjoint subsets $D_1,\ldots,$ and D_m of D, the restriction of f to each D_i, that is, $f|D_i$ is continuous.

Definition 3.1. Let γ be a compact subset of D, such that for each $1 \leq i \leq m$, $\gamma_i = \gamma \cap D_i$ is nonempty and compact, then γ is called a connection with respect to $D_1,\ldots,D_{m-1}$ and D_m.
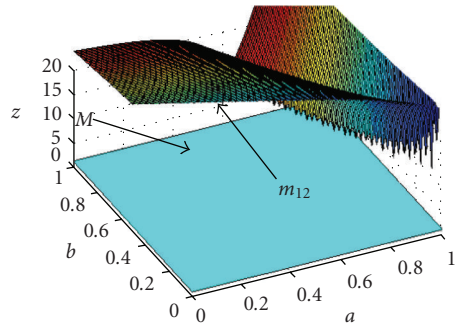
Let F be a family of connections γ's with respect to $D_1,\ldots,D_{m-1}$ and D_m satisfying the following property:

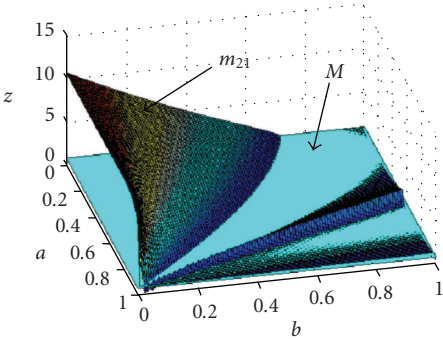$$\gamma \in F \Longrightarrow f(\gamma_i) \in F. \tag{3.1}$$

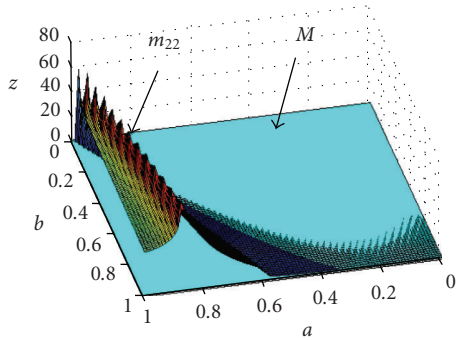Then F is said to be an f-connected family with respect to $D_1,\ldots,D_{m-1}$ and D_m.
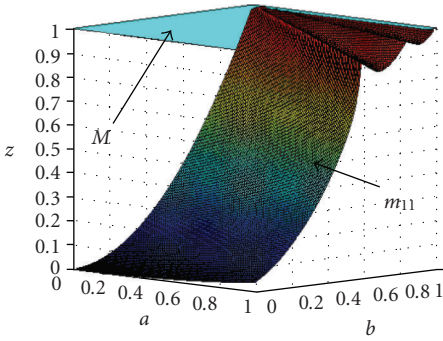
(a) m_{11} as a function of the parameters a and b.

(b) m_{12} as a function of the parameters a and b.

(c) m_{21} as a function of the parameters a and b.

(d) m_{22} as a function of the parameters a and b.

Figure 2.1. The modules of the eigenvalues.

THEOREM 3.2. *Suppose that there exists an f-connected family F with respect to $D_1,\ldots,$ D_{m-1} and D_m. Then there exists a compact invariant set $K \subset D$, such that $f|K$ is semiconjugate to m-shift*

For the proof of this theorem, see [9].

Here the "semiconjugate to the m-shift" is conventionally defined in the following sense. If there exists a continuous and onto mapping

$$h : K \longrightarrow \sum_m, \tag{3.2}$$

such that $h \circ f = \sigma \circ h$, then f is said to be semiconjugate to σ, where σ is the m-shift (mapping) and $\sum_m$ is the space of symbolic sequences to be defined below. Let $S_m = \{1,\ldots,m\}$ be the set of nonnegative successive integer from 1 to m. Let $\sum_m$ be the collection of all one-infinite sequences with their elements of S_m, that is, every element s of $\sum_m$

is of the following form:

$$s = \{s_1,\dots s_m,\dots\}, \quad s_i \in S_m. \tag{3.3}$$

Now consider another sequence $\bar{s}_i \in S_m$.

The distance between s and $\bar{s}$ is defined as

$$d(s,\bar{s}) = \sum_{i=1}^{+\infty} \frac{1}{2^{|i|}} \frac{|s_i - \bar{s}_i|}{|s_i - \bar{s}_i| + 1} \tag{3.4}$$

with the distance defined as (3.4), $\sum_m$ is a metric space, and the m-shift mapping $\sigma : \sum_m \to \sum_m$ is defined as follows [7]:

$$\sigma(s)_i = s_{i+1}, \quad s = \{s_1,\dots s_m,\dots\}. \tag{3.5}$$

For the concept of topological entropy, the reader can refer to [4]. We just recall the result stated in Lemma 3.3, which will be used in this paper.

LEMMA 3.3. *Let X be a compact metric space, and $f : X \to X$ a continuous mapping. If there exists an invariant set $\Lambda \subset X$ such that $f|\Lambda$ is semiconjugate to the m-shift σ, then*

$$h(f) \geq h(\sigma) = \log m, \tag{3.6}$$

where $h(f)$ denotes the entropy of the mapping f. In addition, for every positive integer k,

$$h(f^k) = kh(f). \tag{3.7}$$

A well-known fact is that if the entropy of continuous mapping is positive, then the mapping is chaotic [4].

4. Horseshoes for the mappings

4.1. Horseshoes for the iteration of the mapping p with two saddle points.
Let P denote the mapping corresponding to the parameters $a = 0.24$ and $b = 0.60$, P has two saddle points. With these parameters, we find a quadrangle D with its vertexes: $(-114.2947, -48.3442)$, $(-41.7506, -55.1067)$, $(-46.2846, 63.6224)$ and $(-111.7742, -61.1316)$ by careful computation. Figure 4.1 is the quadrangle D and its image under the fourth iteration of the mapping P(that is P^4). It can be seen from Figure 4.1 that there exist discontinuous points. The resetting (1.3) is responsible for this phenomenon, because not all of the points on the edge of D are reset at the same time.

Four disjoint quadrangles as defined in Definition 3.1 can been constructed, they are d_1, d_2, d_3, d_4. The vertexes' coordinates of d_1, d_2, d_3, d_4 are listed in Table 4.1. Their images under the mapping P^4 are shown in Figure 4.4.

In Figure 4.2, dl_i, are the left sides of d_i, dr_i are the right sides of d_i, $i = 1,2,3,4$. $P^4(dl_i)$ and $P^4(dr_j)$ lie on the left side of dl_1, $i = 1,3$, $j = 2,4$; $P^4(dl_i)$ and $P^4(dr_j)$ lie on the right side of dr_4, $i = 2,4$, $j = 1,3$.

It is easy to see from Figure 4.2 that every line l lying in D and connecting the side dl_1 and dr_4 has nonempty connections with d_1, d_2, d_3 and d_4. Furthermore, $P^4(l \cap d_1)$
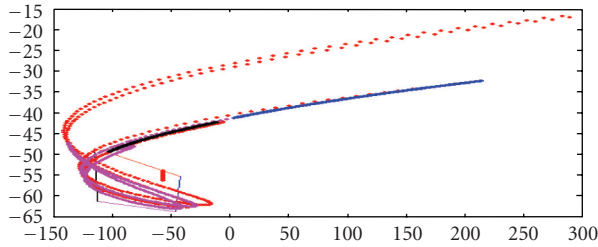
Figure 4.1. The quadrangle D and its image under the mapping P^4.

Table 4.1. The vertexes' coordinates of d_1, d_2, d_3, d_4.

d_1	$(-105.9500, -49.1220)$	$(-99.7860, -49.6970)$	$(-93.1100, -61.8410)$	$(-102.2800, -61.4930)$
d_2	$(-97.9720, -49.8660)$	$(-81.3220, -62.290)$	$(-93.2570, -50.3050)$	$(-92.1270, -61.8790)$
d_3	$(-60.6120, -53.3480)$	$(-56.9850, -53.6870)$	$(-61.3470, -63.050)$	$(-70.1880, -62.7130)$
d_4	$(-53.3580, -54.0250)$	$(-49.3680, -54.3970)$	$(-51.8510, -63.4110)$	$(-58.7280, -63.1490)$

connects dl_1 and dr_4 from the above arguments, $P^4(l \cap d_i)$ also connects dl_1 and dr_4, $i = 2, 3, 4$. Therefore, it is easy to see, in view of Definition 3.1, that there exists a P^4-family with respect to these four subsets d_1, d_2, d_3 and d_4 for the mapping P^4. It follows from Theorem 3.2 that there exists an invariant set K_1 of D, such that P^4 restricted to K_1 is semiconjugated to 4-shift dynamics. Let $h(P^4)$ be the entropy of the mapping P^4, it can be concluded from Lemma 3.3 that $h(P^4) \geq h(\sigma) = \log 4$, consequently the entropy of the mapping P is not less than $(1/2) \log 2$. From above facts, it can be concluded that the mapping P^4 is chaotic.

Because K_1 is an invariant set, every point in K_1 cannot skip out of the quadrangle D under iteration of the mapping P. Then, the resetting has nothing to do with the points in K_1.

4.2. Horseshoes for the iteration of the mapping $\bar{P}$ with a saddle point and a stable equilibrium.

Let $\bar{P}$ denote the mapping corresponding to the parameters $a = 0.64$ and $b = 0.2$, the mapping $\bar{P}$ has a saddle point and a stable equilibrium. With these parameters, we find a quadrangle $\bar{D}$ with its vertexes $(-81.4747, -72.2222)$, $(-39.4470, -84.9708)$, $(-41.2903, -91.8713)$, and $(-83.3180, -83.5673)$ by means of careful computation.

Figure 4.3 is the quadrangle $\bar{D}$ and its image under the sixth iteration of the mapping $\bar{P}$, that is $\bar{P}^6$. The image of $\bar{D}$ under $\bar{P}^6$ has discontinuous part because that not all of the points on the edge of $\bar{D}$ are reset at the same time. Three disjoint quadrangles as defined in Definition 3.1 can also been constructed, they are h_1, h_2, h_3. The vertexes' coordinates of h_1, h_2, h_3 are listed in Table 4.2.

In Figure 4.4, hl_i, are the left sides of h_i, hr_i are the right sides of h_i, $i = 1, 2, 3$. $\bar{P}^6(hl_1)$, $\bar{P}^6(hr_2)$ and $\bar{P}^6(hr_3)$ lie on the left side of hl_1, $\bar{P}^6(hr_1)$, $\bar{P}^6(hl_2)$ and $\bar{P}^6(hl_3)$ lie on the right side of hr_3.
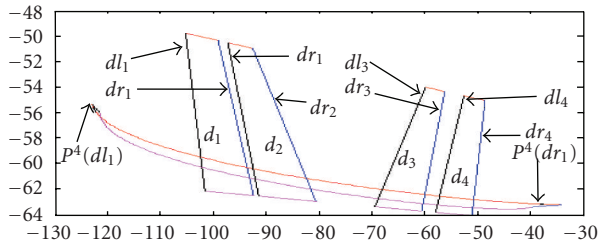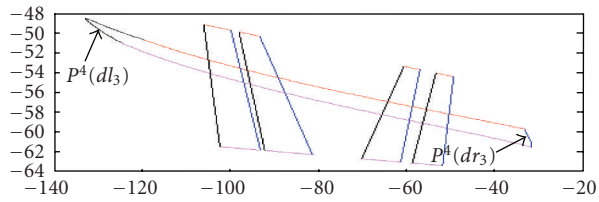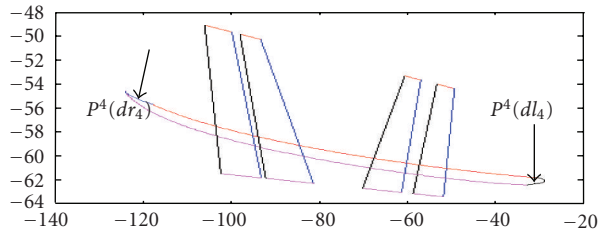
(a) The four disjoint subsets of D and the image of d_1 under the mapping P^4.
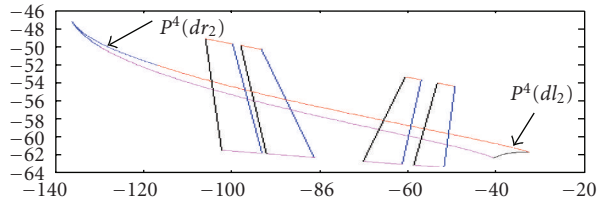
(b) The four disjoint subsets of D and the image of d_2 under the mapping P^4.

(c) The four disjoint subsets of D and the image of d_3 under the mapping P^4.

(d) The four disjoint subsets of D and the image of d_4 under the mapping P^4.

Figure 4.2. The four disjoint subsets of D and their images under the mapping P^4.

It is easy to see from Figure 4.4 that every line l lying in $\bar{D}$ and connecting the side hl_1 and hr_3 has nonempty connections with h_1, h_2, and h_3. Furthermore, $\bar{P}^6(l \cap h_i)$ connects hl_1 and hr_3 from the above arguments, $i = 1, 2, 3$. In view of Definition 3.1, there exists a $\bar{P}^6$-family with respect to these three subsets h_1, h_2, and h_3 for the mapping $\bar{P}^6$. It follows from Theorem 3.2 that there exists an invariant set K_2 of $\bar{D}$, such that $\bar{P}^6$ restricted to K_2
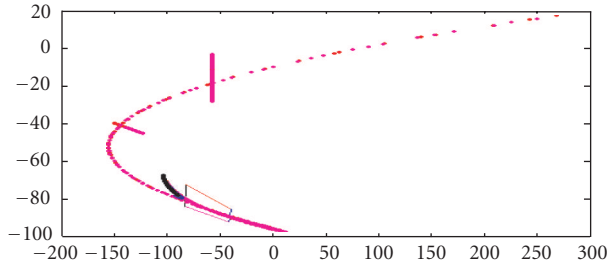
Figure 4.3. The quadrangle $\bar{D}$ and its image under the mapping $\bar{P}^6$.

Table 4.2. The vertexes' coordinates of h_1, h_2, h_3.

h_1	$(-61.9320, -78.1500)$	$(-59.6200, -78.8510)$	$(-65.2460, -87.1380)$	$(-67.9780, -86.5980)$
h_2	$(-58.5700, -79.1700)$	$(-62.0940, -87.7610)$	$(-57.9390, -79.3610)$	$(-62.7240, -87.6360)$
h_3	$(-41.3380, -84.3970)$	$(-39.4470, -84.9708)$	$(-41.2903, -91.8713)$	$(-44.8630, -91.1650)$

is semiconjugated to 3-shift dynamics. Let $h(\bar{P}^6)$ be the entropy of the mapping $\bar{P}^6$, it can be concluded from Lemma 3.3 that $h(\bar{P}^6) \geq h(\sigma) = \log 3$, consequently the entropy of the mapping $\bar{P}$ is not less than $(1/6)\log 3$. The entropy of the mapping $\bar{P}$ is positive, then it can be concluded that the mapping $\bar{P}^6$ is chaotic.

Because K_2 is an invariant set, every point in K_2 cannot skip out of the quadrangle $\bar{D}$ under iteration of the mapping $\bar{P}$. Then, the resetting has nothing to do with the points in K_2.

4.3. Horseshoes for the iteration of the mapping I. The mapping I in [3] is a typical mapping with two saddle points. The mapping can produce a variety of bursting patterns, including those corresponding to IB (intrinsically bursting) and CH (chattering) neocortical neurons. A discussion on chaotic property in this mapping is given in this section.

Let $\hat{P}$ denote the mapping with $I = -99$. As the parameters in (1.1), the mapping $\hat{P}$ has two saddle points. With these parameters, we find a quadrangle $\hat{D}$ with its vertexes $(-47.902, -9.2532)$, $(-28.4005, -9.2532)$, $(-23.3627, -21.6558)$, and $(-53.424, -21.709)$ by means of careful computation.

Figure 4.5 is the image of the quadrangle $\hat{D}$ and its image under the fourth iteration of the mapping $\hat{P}$, that is $\hat{P}^4$. It can be seen from Figure 4.5 that there exist discontinuous points. The reason is the same as that in Section 4.1: the resetting (1.3) is responsible for this phenomenon. Four disjoint quadrangles as defined in Definition 3.1 can also been constructed, they are k_1, k_2, k_3, k_4. The vertexes' coordinates of k_1, k_2, k_3, k_4 are listed in Table 4.3. Their images under the fourth iteration of the mapping $\hat{P}$ are shown in Figure 4.6.

In Figure 4.6, the four quadrangles are k_1, k_2, k_3, k_4 from left to right in turn. kl_i is the left side of k_i, kr_i is the right side of k_i, $i = 1, 2, 3, 4$. $\hat{P}^4(kl_i)$ and $\hat{P}^4(kr_j)$ lie on the left side of kl_1, $i = 2, 4$, $j = 1, 3$; $\hat{P}^4(kl_i)$ and $\hat{P}^4(kr_j)$ lie on the right side of kr_4, $i = 1, 3$, $j = 2, 4$.
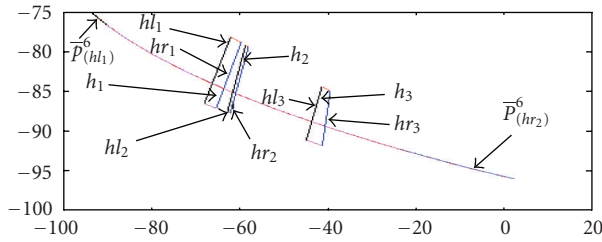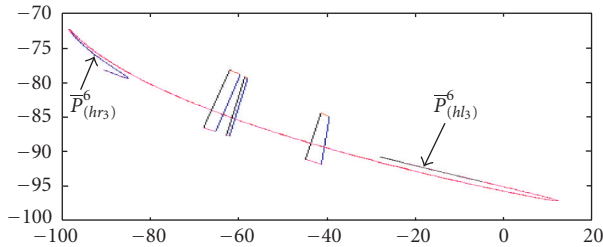
(a) The three disjoint subsets of $\bar{D}$ and the image of h_1 under the mapping $\bar{P}^6$.
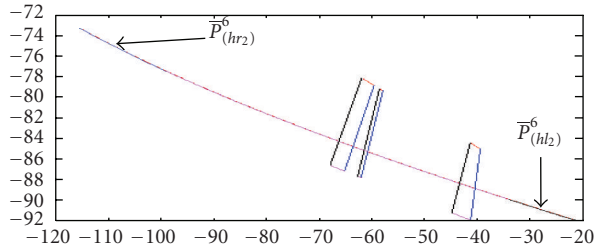
(b) The three disjoint subsets of $\bar{D}$ and the image of h_2 under the mapping $\bar{P}^6$.

(c) The three disjoint subsets of $\bar{D}$ and the image of h_3 under the mapping $\bar{P}^6$.

Figure 4.4. The three disjoint subsets of $\bar{D}$ and their image under the mapping $\bar{P}^6$.

Table 4.3. The vertexes' coordinates of k_1, k_2, k_3, k_4.

k_1	$(-45.172, -9.2532)$	$(-44.879, -9.2532)$	$(-48.915, -21.701)$	$(-49.366, -21.702)$
k_2	$(-42.734, -9.2532)$	$(-42.149, -9.2532)$	$(-45.608, -21.695)$	$(-46.51, -21.697)$
k_3	$(-37.079, -9.2532)$	$(-36.396, -9.2532)$	$(-39.596, -21.685)$	$(-40.648, -21.686)$
k_4	$(-33.568, -9.2532)$	$(-33.178, -9.2532)$	$(-35.688, -21.678)$	$(-36.289, -21.679)$

With the same analysis of the fourth paragraph in Sections 4.1 and 4.2, it can be concluded that there exists a $\widehat{P}^4$-family with respect to these four subsets d_1, d_2, d_3 and d_4 for the mapping $\widehat{P}^4$, and an invariant set K_3 of $\widehat{D}$, such that $\widehat{P}^4$ restricted to K_3 is
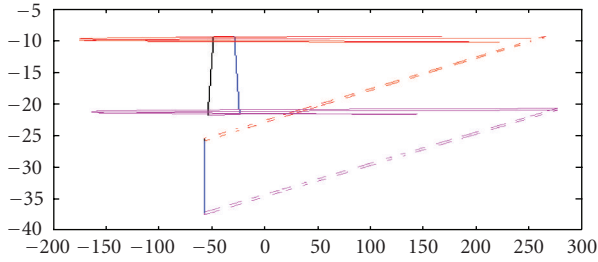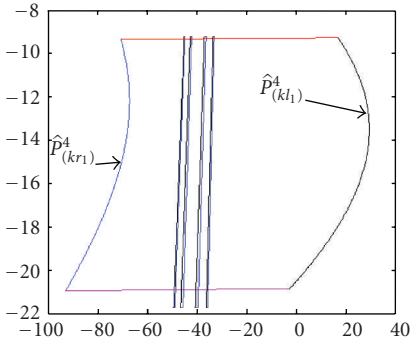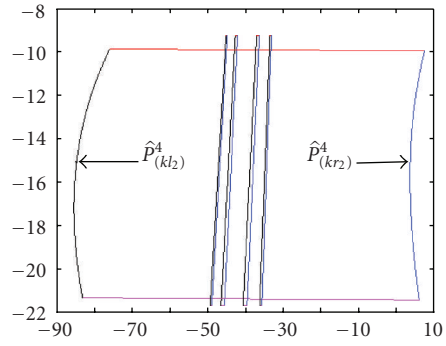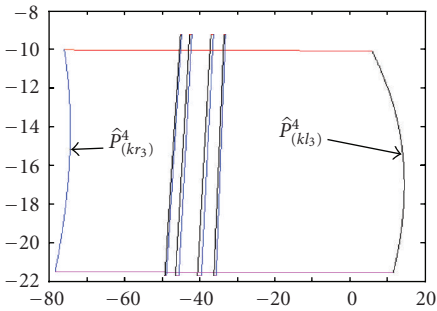
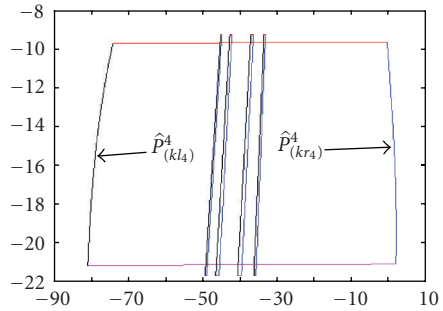Figure 4.5. The quadrangle $\hat{D}$ and its image under the mapping $\hat{P}^4$.

(a) The image of k_1 under the mapping $\hat{P}^4$.

(b) The image of k_2 under the mapping $\hat{P}^4$.

(c) The image of k_3 under the mapping $\hat{P}^4$.

(d) The image of k_4 under the mapping $\hat{P}^4$.

Figure 4.6. The four disjoint subsets of $\hat{D}$ and their images under the mapping $\hat{P}^4$.

semiconjugated to 4-shift dynamics. Let $h(\hat{P}^4)$ be the entropy of the mapping $\hat{P}^4$, it can be concluded from Lemma 3.3 that $h(\hat{P}^4) \geq h(\sigma) = \log 4$, consequently the entropy of the mapping $\hat{P}$ is not less than $(1/2)\log 2$. From above facts, it can be concluded that the mapping $\hat{P}^4$ is chaotic.

Because K_3 is an invariant set, every point in K_3 cannot skip out of the quadrangle $\hat{D}$ under iteration of the mapping $\hat{P}$. Then, the resetting has nothing to do with the points in K_3.

5. Conclusion

Studying networks of bursters in neural systems poses challenging mathematical problems. A bursting dynamics of mappings has been investigated in this paper. Based on the stability analysis of the system's equilibria with various parameters, we study three mappings of the system, that is P^4, $\bar{P}^6$ and $\hat{P}^4$. We show that the mappings are chaotic by giving a rigorous verification for existence of horseshoes in these mappings. We prove that the mapping $\bar{P}^6$ is semiconjugate to the 3-shift mapping, the mapping P^4 and $\hat{P}^4$ are semiconjugate to the 4-shift mapping. Then, the mappings P^4, $\bar{P}^6$, and $\hat{P}^4$ are chaotic.

Acknowledgments

References

[1] B. Cazelles, M. Courbage, and M. Rabinovich, *Anti-phase regularization of coupled chaotic maps modelling bursting neurons*, Europhysics Letters **56** (2001), no. 4, 504–509.

[2] G. de Vries, *Bursting as an emergent phenomenon in coupled chaotic mappings*, Physical Review E. Statistical, Nonlinear, and Soft Matter Physics **64** (2001), no. 5, 051914.

[3] E. M. Izhikevich and F. Hoppensteadt, *Classification of bursting mappings*, International Journal of Bifurcation and Chaos in Applied Sciences and Engineering **14** (2004), no. 11, 3847–3854.

[4] C. Robinson, *Dynamical Systems. Stability, Symbolic Dynamics, and Chaos*, Studies in Advanced Mathematics, CRC Press, Florida, 1995.

[5] N. F. Rulkov, *Regularization of synchronized chaotic bursts*, Physical Review Letters **86** (2001), no. 1, 183–186.

[6] ———, *Modeling of spiking-bursting neural behavior using two-dimensional map*, Physical Review E. Statistical, Nonlinear, and Soft Matter Physics **65** (2002), no. 4, 041922, 9.

[7] S. Wiggins, *Introduction to Applied Nonlinear Dynamical Systems and Chaos*, Texts in Applied Mathematics, vol. 2, Springer, New York, 1990.

[8] X.-S. Yang, *Metric horseshoes*, Chaos Solitons Fractals **20** (2004), no. 5, 1149–1156.

[9] X.-S. Yang and Y. Tang, *Horseshoes in piecewise continuous maps*, Chaos Solitons Fractals **19** (2004), no. 4, 841–845.

Yan Huang: Department of Mathematics, Huazhong University of Science and Technology, Wuhan 430074, China
Current address: Department of Control Science and Engineering, Huazhong University of Science and Technology, Wuhan 430074, China
E-mail address: huangyan2323@163.com

Xiao-Song Yang: Department of Mathematics, Huazhong University of Science and Technology, Wuhan 430074, China
E-mail address: yangxs@cqupt.edu.cn